

Aerodynamic Design for Supersonic Nozzles of Arbitrary Cross Section

A. Haddad* and J. B. Moss†

Cranfield Institute of Technology, Bedford, England, United Kingdom

A comparatively simple method for obtaining wall contours of supersonic nozzles of arbitrary exit cross sections from readily determined axisymmetric flows is presented. An initial axisymmetric flowfield is calculated using the method of characteristics in two dimensions from which the desired three-dimensional shape may be generated by specifying the appropriate cross section at the streamwise station giving the required overall nozzle length and exit Mach number. The describing points on the perimeter of this section are traced along corresponding streamlines back to the throat. The stream sheets formed by these streamlines then define the new nozzle contour. Elliptical and two-dimensional wedge-shaped nozzles are designed using this approach, and comparisons are reported between detailed finite-difference flowfield predictions and experimental measurement.

I. Introduction

A VARIETY of aerospace applications require three-dimensional supersonic internal flow calculations. These include, among others, nozzles for propulsion engines having nonsymmetric area constraints and for high-speed aircraft, which increasingly require careful airframe/propulsion system integration.

Predictive methods for nozzle flows of varying complexity may each play an important role in the design process from initial concept to detailed aerothermodynamic simulation and performance evaluation. Computational methods which solve such complex three-dimensional flows are becoming more widely accessible. However, special techniques are usually adopted to suit specific cases and there is inevitably a tendency toward the ever greater specialization of generalized methods. Such sophistication creates substantial difficulty for the non-specialist user in both understanding the program and preparing the necessary input. Lengthy operating and turn-around times result, and consequently high costs are incurred. Furthermore, significant technological deficiencies are still associated with such methods—one of the most important being in the area of geometric modeling. Computer codes based on the finite-difference method, for example, are generally tailored to a specific grid topology. Although body geometries that fit this particular topology may be analyzed accurately, a variety of problems accompany the severe loss of grid orthogonality, which often occurs as a grid is body fitted about a new geometry not suited to the particular topology. Grid refinement, by increasing the number of cells or redesigning the grid geometry, may reduce the effects of nonorthogonality, but these approaches are often costly and inconvenient. This must vitiate much of the attraction in computational flow simulation, which lies in the alternative presented to time-consuming and expensive hardware demonstration or rig testing, particularly in relation to initial design and often involving the investigation of a range of competing geometries.

The objective of the present research is the development of a simple and reliable method for calculation of supersonic internal flows having complex shapes and the preliminary de-

sign of representative three-dimensional supersonic nozzles based on such computations.

II. Approach

The method developed is simply based on three key features of inviscid axisymmetric flows.

1) The streamlines of such flows lie in planes through the streamwise axis.

2) The flow in any one such plane is the same as that in any other.

3) The stream sheets (formed by the preceding streamlines) generate surfaces across which there is no flow and which may be replaced by solid boundaries to a first approximation.

These characteristics will be exploited in order to calculate comparatively simply the nozzle or inlet having the desired shape. First, the axisymmetric nozzle having the desired length and Mach number is computed. Then, choosing the desired cross-section shape at the exit, the streamlines which pass through its periphery are located and traced back to the throat. The stream sheets formed by these streamlines then constitute the walls of the desired nozzle.

Two three-dimensional nozzles, one of elliptical cross section and a two-dimensional wedge, have been designed using this approach. The detailed procedures and the validation of the aerodynamic design are described in the following sections.

III. Nozzle Designs

Axisymmetric Design

Inviscid flow calculations were carried out using the method of characteristics (see Zucrow and Hoffman²) and based in particular on the scheme proposed by Sauer.³ The axisymmetric nozzle, from which the elliptical nozzle was developed subsequently, is contoured, comprising a throat formed by two circular arcs of different radii of curvature. The upstream throat radius of curvature was equal to two throat radii. The circular arc downstream of the throat was joined to it tangentially; this in turn was continuous in the first derivative at an attachment point to a simulated quadratic polynomial wall, responsible for further downstream expansion (see Fig. 1).

The attachment point (x_a, y_a) is readily established from the throat radius y_t , the downstream radius of curvature R_{td} , and the attachment angle A_a , namely

$$x_a = R_{td} \sin A_a$$

$$y_a = y_t + R_{td}(1 - \cos A_a)$$

Received Oct. 20, 1988; revision received Aug. 23, 1989. Copyright © 1990 by the American Institute of Aeronautics and Astronautics, Inc. All rights reserved.

*Research Student, School of Mechanical Engineering.

†Professor, School of Mechanical Engineering.

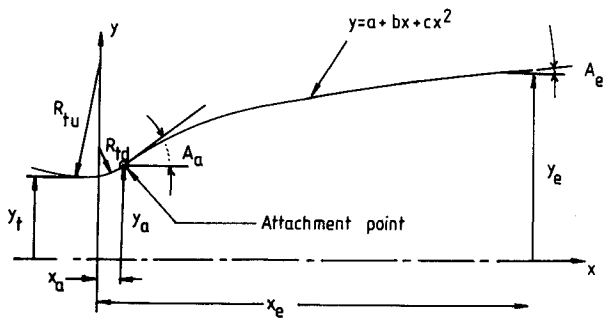


Fig. 1 Axisymmetric contoured nozzle configuration.

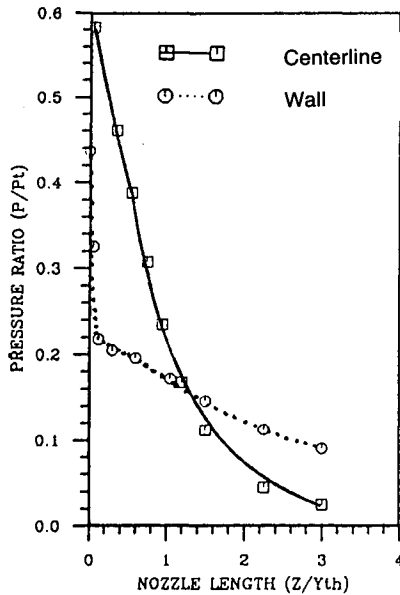


Fig. 2 Comparison of the wall and centerline pressure ratios as a function of axial position in the axisymmetric contoured nozzle.

Two options are then available to determine the coefficients in the second-order polynomial depending on whether the nozzle length x_e or the exit radius y_e are prescribed; for example, the constraints

$$y(x_a) = y_a, \left(\frac{dy}{dx}\right)_{x_a} = \tan A_a, \left(\frac{dy}{dx}\right)_{x_e} = \tan A_e$$

permit the straightforward determination of the coefficients a , b , and c .

The axisymmetric nozzle, from which the two-dimensional wedge was designed, was conical. The throat again comprised two circular arcs, the one downstream of the throat joined to a divergent wall of 2 deg included half-angle.

The flows were assumed to be steady, compressible, and irrotational. The elliptical and wedge nozzles were designed to expand the flows from sonic velocity to average Mach numbers (based on area) of 2.4 and 1.4, respectively. The method of characteristics solutions for the two axisymmetric nozzles are shown in Figs. 2 and 3. Both the nozzle wall and centerline pressures are plotted. Because of the higher value of the attachment angle of the axisymmetric-for-elliptic nozzle (15 deg), a substantially sharper expansion is exhibited in the vicinity of the throat in this case.

Given the inviscid nature of these calculations and the intention, within the strategy outlined in the preceding section, to replace stream-sheet surfaces by solid walls, the boundary-layer development on the nozzle walls was estimated using a method based on the work of Herring and Mellor.⁴

Outer flow boundary conditions to be imposed on the viscous boundary layer were determined from the inviscid flow-field computed using the method of characteristics. Figures 4 and 5 show the corrections needed (in terms of the displacement thickness) in order to include the viscous effects on the nozzle walls.

These results show that the corrections needed are indeed very small ($\approx 0.3\%$ in terms of δ^*/R). Furthermore, the area occupied by the boundary layer typically did not exceed 0.7% of the total cross-sectional area, resulting in values of the blockage coefficients, defined as the ratio of the inviscid flow area to the total flow area, exceeding 0.99. In view of these results, it is appropriate to neglect to first-order viscous effects on both axisymmetric configurations investigated.

Three-Dimensional Design

In order to transform the axisymmetric nozzles, computed using this procedure, to more general nonaxisymmetric ones,

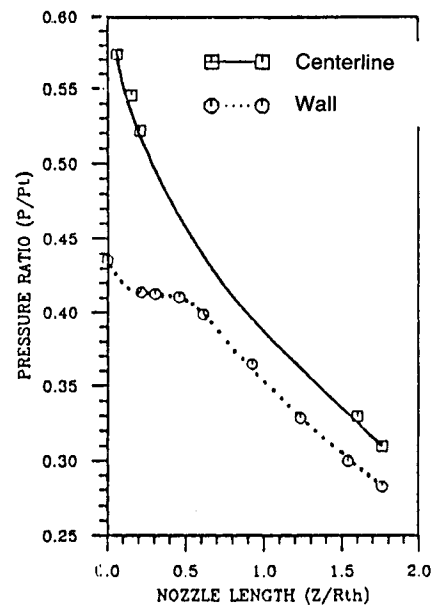


Fig. 3 Comparison of the wall and centerline pressure ratios as a function of axial position in the axisymmetric conical nozzle.

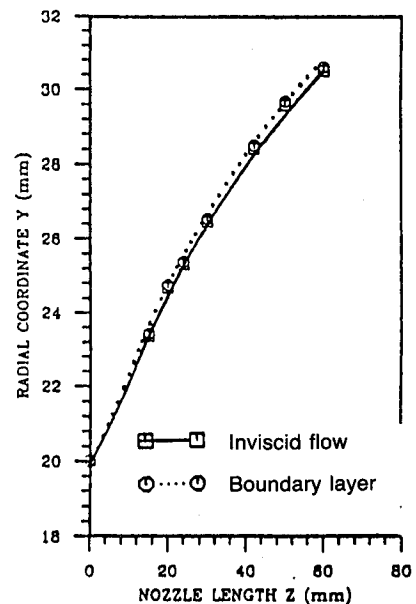


Fig. 4 Boundary-layer development in terms of the displacement thickness within the axisymmetric contoured nozzle.

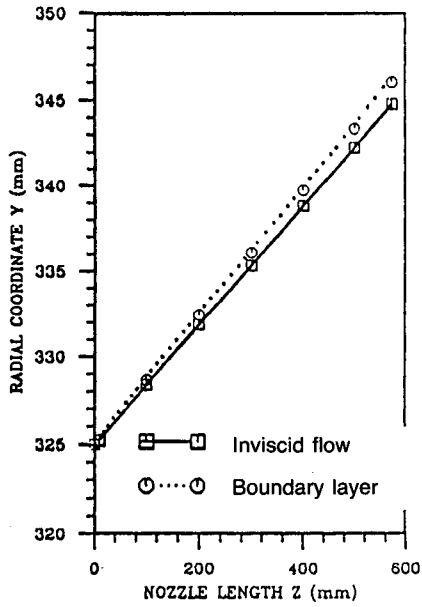


Fig. 5 Boundary-layer development in terms of the displacement thickness within the axisymmetric conical nozzle.

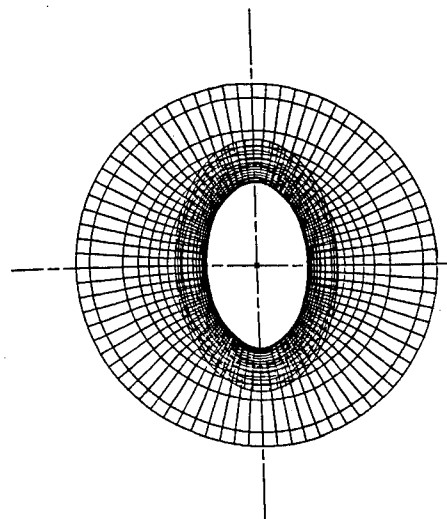
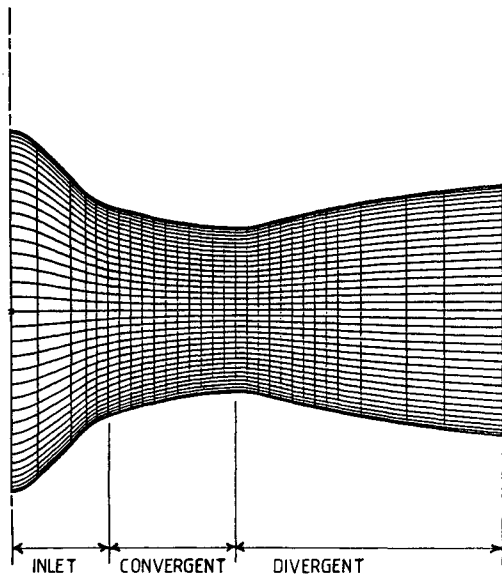


Fig. 6 Elliptical nozzle.

the desired nonsymmetrical shapes are chosen at the exit cross section. The streamlines, whose intersection with the exit plane defines the particular profile shape, are then calculated and traced back to the throat. These have been determined by integrating directly the axisymmetric stream function inferred from the local flow properties of density and velocity given by grid node values from the characteristics solution. The stream sheets formed by the streamlines then constitute the walls of the desired nozzle.

The elliptical nozzle (see Fig. 6) was chosen because it is sufficiently simple to admit ready experimental verification and might be viewed as typical of the type of nozzles having application in integral rocket-ramjet or scramjet powerplants. Figure 7 shows the exit cross-sectional shapes of the initial axisymmetric and required elliptical configurations. The equation of the ellipse was determined by selecting the ratio of the major axis to the minor axis to be $b/a = 1.5$.

The two-dimensional wedge nozzle illustrates the newer technology propulsion nozzles which are to be integrated into future military aircraft. Figure 8 again compares the initial axisymmetric and the subsequent two-dimensional shapes at the exit cross section. The final shape is defined by the points, $A, B_1, B_2, B_3,$ and C . The coordinates of these stations were determined by selecting the ratio of the internal radius y_i to the external radius y_e to be 0.9.

IV. Results and Discussion

In order to demonstrate the performance of nozzles designed in this manner, detailed analysis of the flowfield within the nonaxisymmetric nozzles was performed using both finite-difference flowfield simulation and experimental testing of the elliptical nozzle.

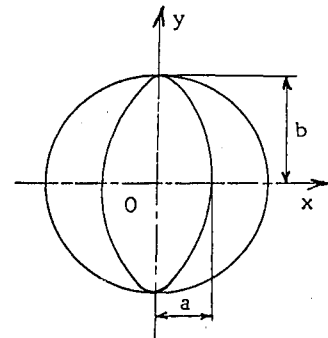


Fig. 7 Exit cross-sectional shapes of the axisymmetric and elliptical nozzles.

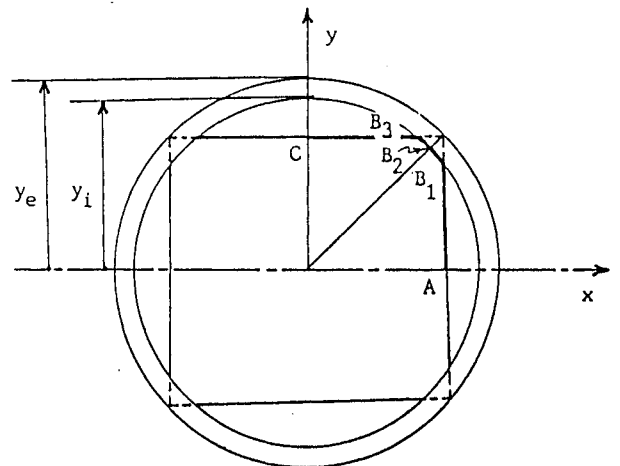


Fig. 8 Exit cross-sectional shapes of the axisymmetric and two-dimensional wedge nozzle.

PHOENICS⁶ (Parabolic, Hyperbolic or Elliptic Numerical Integration Code Series), a general purpose computational fluid dynamics (CFD) code, was used to simulate the three-dimensional flow. The calculation was initiated at the throat using the same initial data as employed for the axisymmetric flows and restricted to the expanding supersonic flow. The necessary computational grids describing the two configurations were generated by the Internal Design Engineering Analysis Software (I-Deas) Supertab module.⁵ A more finely resolved mesh was employed in the vicinity of the throat where property gradients are expected to be higher.

Elliptical Nozzle

Figure 9 represents an isometric view of the cross sections and boundaries for one quadrant of the elliptical nozzle. Fifty-two streamlines were used to generate the whole elliptical configuration. The calculations were carried out at 15 cross sections starting from the throat. The initial conditions were prescribed by the stagnation pressure and temperature, and the inlet static pressure was established from the prescribed mass flow rate (assumed to be air and conforming to the experimental test conditions described later) and the nozzle inlet dimensions. A smooth transition is effected between the elliptical throat and upstream axisymmetric supply by circular arc pro-

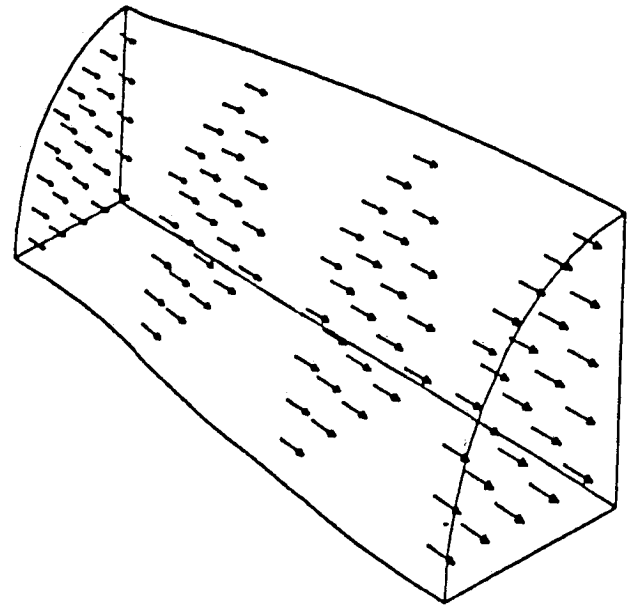


Fig. 11 Velocity vectors at cross sections of the elliptical nozzle.

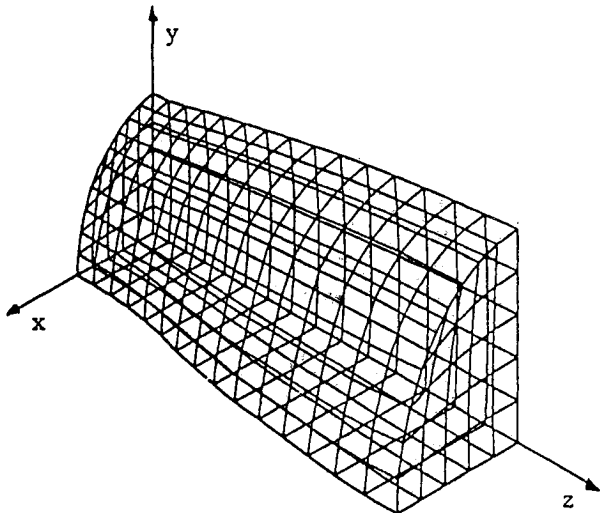


Fig. 9 Isometric view of the elliptical nozzle.

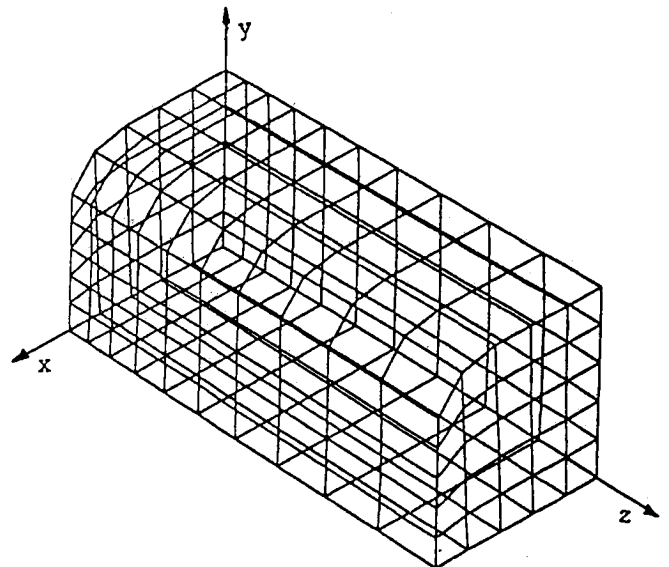


Fig. 12 Isometric view of the two-dimensional wedge nozzle.

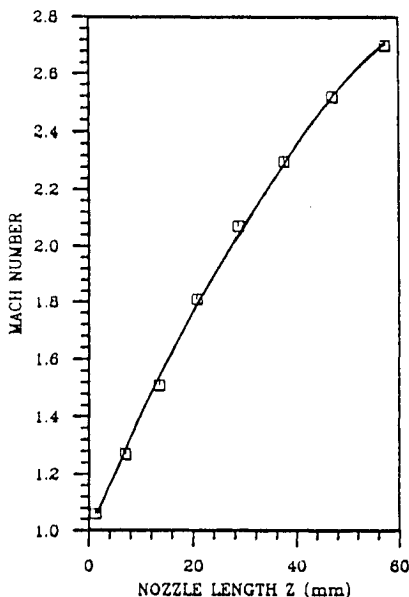


Fig. 10 Mach number distribution along the centerline of the elliptical nozzle.

Table 1 Study of the performances of the elliptical nozzle compared to its axisymmetric contoured counterpart

	Thrust, N	\dot{m} , kg/s	C_D	T/\dot{m} , m/s	M_e
Elliptical nozzle	1578	2.25	1.24	701	2.47
Axisymmetric nozzle	2470	2.80	1.31	882	2.36

files. Figure 10 shows the Mach number distribution along the centerline and Fig. 11 the velocity field resulting from the flowfield computations. The flow is shown to accelerate smoothly and uniformly along the nozzle.

The thrust, thrust coefficient, and exit Mach number produced by the elliptical nozzle and its axisymmetric counterpart are compared in Table 1. When differences in nozzle cross section and mass flow are taken into account, in the form of specific thrust, the axisymmetric nozzle performance – based on the method of characteristics solution – is significantly better than that of the elliptical nozzle – based on the CFD simulation.

Such comparisons are, however, potentially misleading if we recall that the prescription of uniform exit static pressure,

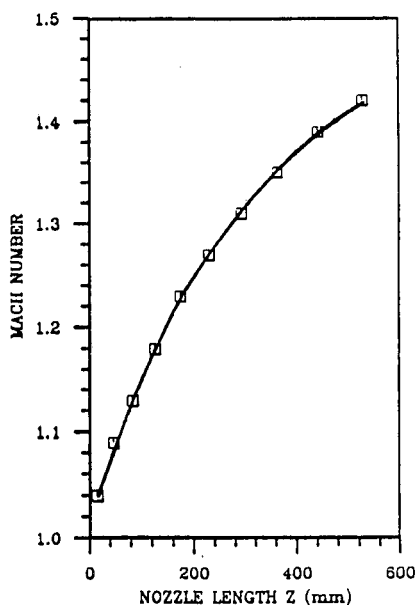


Fig. 13 Mach number distribution along the centerline of the two-dimensional wedge nozzle.

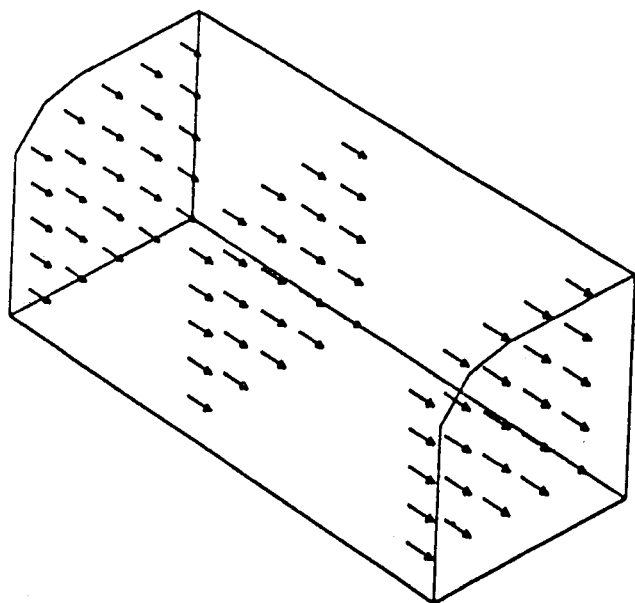


Fig. 14 Velocity vectors at cross sections of the two-dimensional wedge nozzle.

employed in the flowfield simulation, is not attained in practice. Further discussion of this aspect is deferred until the comparison with experiment is reported.

Two-Dimensional Wedge Nozzle

Among the more promising design techniques proposed to enhance the performance of fighter aircraft are concepts incorporating two-dimensional wedge nozzles into jet engines.

The two-dimensional nozzle contour used to demonstrate the present method was generated by 16 streamlines. The flowfield computation was performed at ten successive cross sections starting from the throat. An isometric view of the nozzle is presented in Fig. 12. The corresponding axial Mach number distributed along the centerline and cross-sectional velocity distributions are shown in Figs. 13 and 14, respectively.

At lower power settings, the overall area ratios of such nozzles are fairly modest, and the expansion process within these configurations takes place very gradually. Figure 15 represents the solution along the centerline. The discrepancy be-

tween the axisymmetric and three-dimensional, nonaxisymmetric cases, calculated using the method of characteristics and finite-difference code respectively, is small ($\leq 3\%$). The comparatively gradual pressure drop reflects the low value of the divergence angle corresponding to the cruise conditions at which the nozzle was designed. A modest performance advantage is again implied for the axisymmetric nozzle in Table 2, but the comparisons might equally be interpreted as an encouraging test for general purpose CFD simulation in such applications.

Comparison with Experimental Data

In order to test the validity of the design method experimentally, and as a secondary task shed light on the different prediction methods, a nozzle was constructed to the specifications of the elliptical nozzle and cold-flow tested with air as the flowing medium. The static pressure was measured at different equally spaced stations (5-mm separation) along the centerline and the exit minor and major axes. Two purpose-designed and manufactured probes¹ were used to perform the tests. A conventional conical probe of 8 deg included angle was used in the exit plane, and the axial static pressure variation was measured using a hypodermic centerbody probe (see Fig. 16). The tests were run at a stagnation pressure of 235 psia ($1.62 \times 10^6 \text{ Nm}^{-2}$) with expansion to ambient atmospheric pressure. Figure 17 compares the three-dimensional theoretical predictions for the pressure distribution along the centerline and the measured values.

Agreement between the two solutions is good except at points of near-discontinuous rates of change in flow properties. Point A of Fig. 17 is such a point. It represents the station on the nozzle axis at which the first expansion wave from the wall reaches the axis. The discretized, three-dimensional calculation smooths out such variations. The degree of grid refinement necessary to explore such features was considered inappropriate to this preliminary study.

Table 2 Study of the performance of the two-dimensional wedge nozzle compared to its axisymmetric conical counterpart

	Thrust, N	\dot{m} , kg/s	C_D	T/\dot{m} , m/s	M_e
Two-dimensional	62,275	90	0.93	692	1.41
Axisymmetric nozzle	105,868	130	0.98	814	1.44

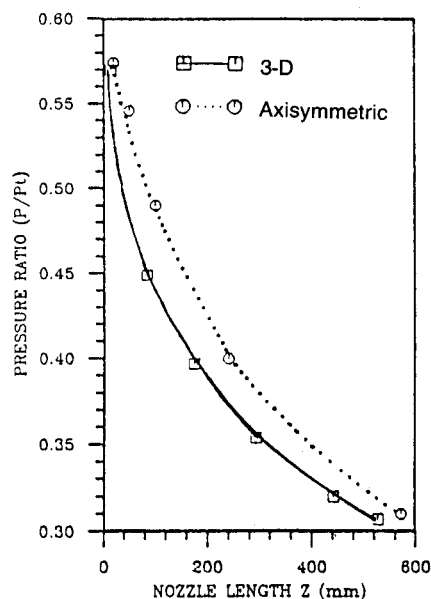


Fig. 15 Comparison of calculated centerline pressure ratios as a function of axial position in the axisymmetric conical (method of characteristics) and two-dimensional wedge nozzle (CFD prediction).

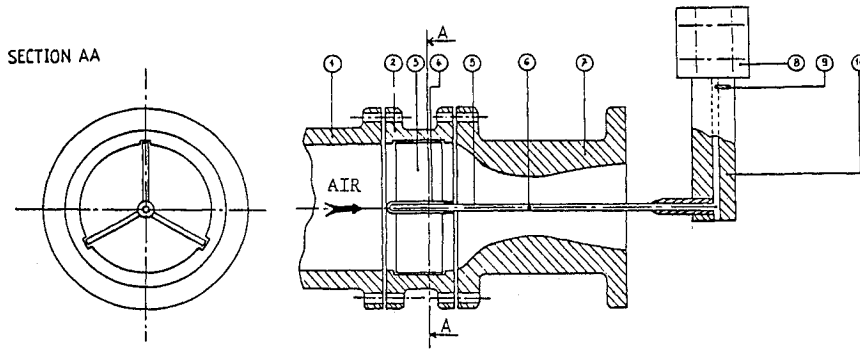


Fig. 16 Layout of the experimental apparatus showing the hydrodermic center-body probe in position.

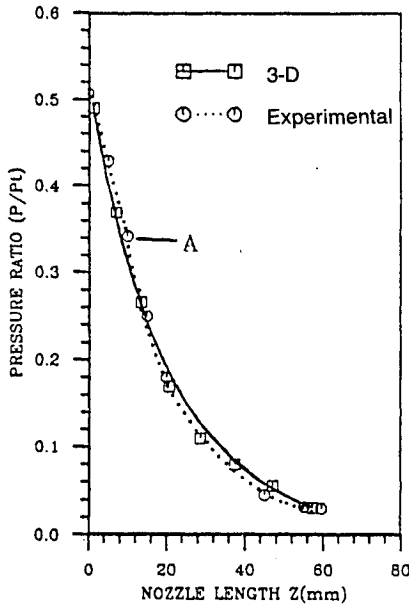


Fig. 17 Comparison between theoretical and experimental pressure ratios along the centerline of the elliptical nozzle.

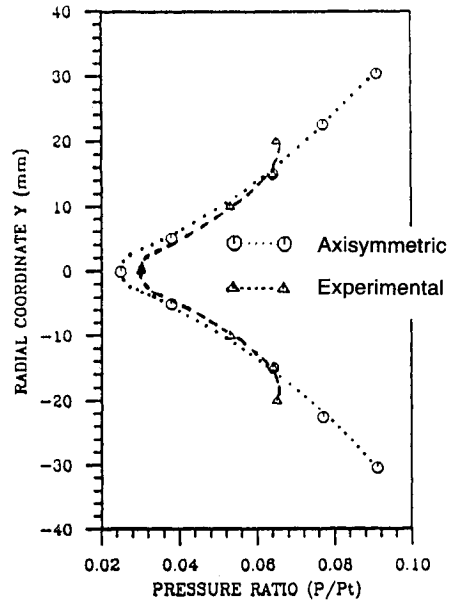


Fig. 19 Exit cross-section comparisons between axisymmetric (method of characteristics) predictions and measurements along minor axis of elliptical nozzle (40-mm length).

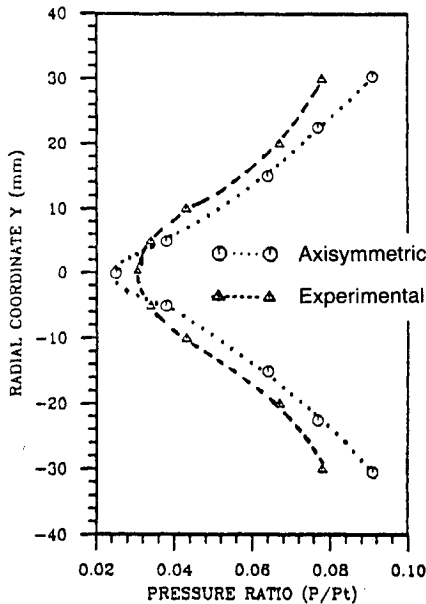


Fig. 18 Exit cross-section comparisons between axisymmetric (method of characteristics) predictions and measurements along major axis of elliptical nozzle.

Static pressure measurements were also performed along the major and minor axis of the exit cross section. The results are compared with the solution obtained along the exit cross section of the axisymmetric configuration, from which the actual elliptical nozzle was designed subsequently, in Fig. 18 for the major axis ($b = 30$ mm) and Fig. 19 for the minor axis ($a = 20$ mm).

The measurements confirm the restrictive nature of the modeling assumption of uniform static pressure distribution at exit suggesting a difference from the centerline at the extremities of major and minor axes of between 6 and 8%. Dramatic boundary-layer growth in the vicinity of the highly curved walls on the major axis is not indicated, however, despite the major departure of this wall from the axisymmetric stream surfaces of the original nozzle flow.

V. Conclusion

A simple method for determining three-dimensional contours from axisymmetric flows has been developed and shown to produce encouraging results. The technique has been applied to the design of two nonaxisymmetric propulsion nozzles and has generated satisfactory configurations. Detailed three-dimensional simulation of the flowfield within the designed nozzles has been performed using a general purpose CFD code

and compared with the experimental testing in the case of a nozzle of elliptical cross section.

The nozzle flow is shown to expand smoothly despite the significant departure of the contours investigated from the axisymmetric property distributions from which they are generated. The flowfield simulation is shown to plausibly reproduce the evolution of static pressure distribution along the nozzle, although some significant discrepancies are observed relative to wall static pressure predicted by the method of characteristics for the originating axisymmetric flows.

These more detailed analyses of the internal flow do, however, lend further credibility to the procedure outlined for the preliminary design of supersonic nozzles of arbitrary cross-sectional shape.

Acknowledgments

The authors are pleased to acknowledge helpful formative discussions with Leo Townsend, and assistance in the model

manufacture from the Royal Aerospace Establishment, Bedford, England, United Kingdom.

References

- ¹Haddad, A., "Supersonic Nozzle Design of Arbitrary Cross-Section," Ph.D. Thesis, Cranfield Inst. of Technology, Bedford, England, 1988.
- ²Zucrow, M. J., and Hoffman, J. D., *Gas Dynamics*, Wiley, New York, 1976.
- ³Sauer, R., "General Characteristics of the Flow Through Nozzles at Near Critical Speeds," NACA TM-1147, 1947.
- ⁴Herring, H. J., and Mellor, G. L., "Computer Program for Calculating Laminar and Turbulent Boundary Layer Developments in Compressible Flow," NASA CR-2068, 1972.
- ⁵"I-Deas Supertab - Engineering Analysis, Pre- and Post-Processing," Structural Dynamics Research Corp., 1986.
- ⁶Rosten, H. I., and Spalding, D. B., "Phoenix Beginner's Guide and User's Manual," Concentration Heat and Momentum, Ltd., London, CHAM Rept. TR/100, 1986.

*Recommended Reading from the AIAA
Progress in Astronautics and Aeronautics Series . . .*



Single- and Multi-Phase Flows in an Electromagnetic Field: Energy, Metallurgical and Solar Applications

Herman Branover, Paul S. Lykoudis, and Michael Mond, editors

This text deals with experimental aspects of simple and multi-phase flows applied to power-generation devices. It treats laminar and turbulent flow, two-phase flows in the presence of magnetic fields, MHD power generation, with special attention to solar liquid-metal MHD power generation, MHD problems in fission and fusion reactors, and metallurgical applications. Unique in its interface of theory and practice, the book will particularly aid engineers in power production, nuclear systems, and metallurgical applications. Extensive references supplement the text.

TO ORDER: Write, Phone, or FAX: AIAA c/o TASC0,
9 Jay Gould Ct., P.O. Box 753, Waldorf, MD 20604
Phone (301) 645-5643, Dept. 415 ■ FAX (301) 843-0159

Sales Tax: CA residents, 7%; DC, 6%. For shipping and handling add \$4.75 for 1-4 books (call for rates for higher quantities). Orders under \$50.00 must be prepaid. Foreign orders must be prepaid. Please allow 4 weeks for delivery. Prices are subject to change without notice. Returns will be accepted within 15 days.

1985 762 pp., illus. Hardback
ISBN 0-930403-04-5
AIAA Members \$59.95
Nonmembers \$89.95
Order Number V-100